

Protein Crystallization: Contribution of Small Angle X ray Scattering (SAXS).

F. Bonneté, N. Ferté, J. P. Astier, S. Veessler

CRMCN-CNRS, Campus de Luminy, Case 913, 13288 Marseille Cedex 9

Abstract. Small Angle X-ray Scattering (SAXS) experiments together with crystallization experiments have shown the importance of studying macromolecular associations and interactions involved in nucleation and crystal growth mechanisms. In the study by SAXS of Bovine pancreatic trypsin inhibitor (BPTI) and *Aspergillus flavus* Urate oxidase (UOX) in crystallization conditions, we characterize the crystal growth unit, which is a decamer in the case of BPTI and a tetramer in the case of UOX. We study interactions in solution, showing that salt, added alone to small protein solutions, is efficient to induce attractive interactions leading to crystallization, whereas for large proteins, the addition of non absorbing polymers is necessary to induce attractive interactions, which are characterized by negative values of second virial coefficient (A_2).

1. INTRODUCTION

While it was long supposed that, since each biological macromolecule has a unique amino acid sequence, it also has its own crystallization condition. In fact each macromolecule can have different solubility as a function of physicochemical parameters leading to different crystallization conditions. This depends on each biological object and particularly on its stability, i.e. its ability to maintain its structure in different physicochemical environments, and also on its purity and its monodispersity. To date, the determination of phase diagrams and solubility curves has cost too much in terms of material and time, and crystallization conditions have generally been determined by trial-and-error methods. Since the 90's, a new approach to crystallization studies has been developed: studying molecular interactions in solution by scattering techniques [1-7]. Indeed, whatever their characteristics (size, oligomeric state, compactness, surface charges), biological macromolecules in aqueous solutions or physiological environment are subject to similar forces (van der Waals, coulombic, steric...). Biological macromolecules can be effectively studied by Small angle X-ray scattering (SAXS) in solution since having dimensions from about one to a few hundred nanometer. Such studies make it possible to determine the particle form factor (size and shape of the particle in solution) and the structure factor as a function of various physicochemical parameters and to access, by numerical simulation, pair potentials between particles and therefore the distribution of particles in solution. This physics, initially developed in the colloid and polymer field to determine phase diagram, is now successfully applied to biological macromolecules to account for macroscopic phenomena such as solubility, liquid-solid or liquid-liquid phase separations. First SAXS experiments performed on lysozyme in crystallization conditions have shown a close correlation between the increase in attractive interaction and the decrease in solubility leading to crystallization, when salts are added [3, 6]. The quantification of mean interaction forces by the second virial coefficient A_2 (positive A_2 value for repulsive interactions and negative A_2 value for attractive interactions) avoids the determination of solubility by lengthy trial-and-error experiments [1, 4].

In this review we present SAXS experiments, performed on two model systems of different sizes: Bovin pancreatic trypsin inhibitor (BPTI, MW = 6511 Da) and *Aspergillus flavus* Urate oxidase (UOX, MW = 128000 Da) (Da=g/mol). First, we measure the macromolecule form factor as a function of different physicochemical parameters in order to characterize molecules in solution involved in the crystallization mechanism. Then we determine second virial coefficients, in order to characterize attractive interactions leading to crystallization conditions.

The study of the two protein form factors in crystallization conditions allows us to characterize the growth unit, which is a decamer in the case of BPTI and the native tetramer in the case of UOX. The study of interactions in solution has shown that, adding salt alone to BPTI solutions is efficient to induce attractive interactions leading to crystallization, whereas for large proteins (UOX) non absorbing polymers must be added to induce attractive interactions. Furthermore the second virial coefficients corresponding to crystallization conditions obtained for UOX are in a limited negative range.

2. THEORETICAL BACKGROUND

SAXS is a suitable technique to characterize macromolecules in ideal or diluted solutions and to measure second virial coefficients in the case of concentrated solutions of macromolecules in mutual interaction. It has already been well described in numerous books [8-11].

Mathematically, monodisperse solutions of quasi-spherical particles can be described as the convolution of a motif representing the protein and of the distribution of the particles in solution and schematically represented in Figure 1:

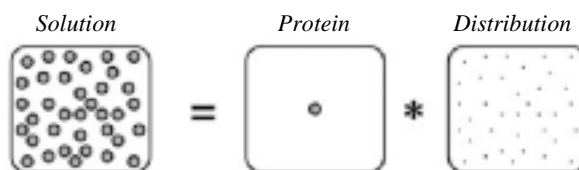


Figure 1. Schematic representation of a solution of macromolecules described mathematically as the convolution product of a particle shape and a particle distribution.

The X-ray scattering curves, $I(c,s)$, can be therefore written as the product of the form factor, $I(0,s)$ (i.e. the scattered intensity of one particle) by the structure factor, $S(c,s)$, which depends on the particle distribution:

$$I(c,s) = I(0,s) \cdot S(c,s) \quad (1)$$

where s is the scattering vector ($s=2\sin\theta/\lambda$), θ the half of the scattering angle and c the macromolecule concentration in g/cm^3 .

2.1 SAXS: structure of the macromolecule in solution

The form factor (i.e. the intensity recorded at low concentration in the limit of a meaningful signal) gives information on the size and the shape of the particle. It can be analyzed in terms of radius of gyration of the particle, R_g , if $2\pi R_g s < 1$ by using the Guinier approximation [8]:

$$I(c \rightarrow 0, s) = I(0,0) \cdot \exp \left\{ -\frac{4\pi^2}{3} R_g^2 s^2 \right\} \quad (2)$$

The extrapolation of the Guinier plot, i.e. the plot of $\text{Log } I(c,s)$ as a function of s^2 , to the s -origin makes it possible to determine the origin $I(0,0)$ and the slope, which gives rise respectively to the molecular weight and the radius of gyration of the particle in solution.

In the case of polydisperse solutions or mixtures of globular particles of number concentration n_i , the total scattered intensity is given by:

$$I(0, s) = \sum_i n_i I_i(0) \quad (3)$$

Such an analysis of scattering patterns can be used to characterize intermediates in the crystallization process.

2.2 SAXS: interactions in solution and second virial coefficient

The structure factor, $S(c, s)$, obtained from the scattered intensity at high concentrations divided by the form factor, gives information on interactions between particles in solution. It depends on the pair distribution function by:

$$S(c, s) = 1 + \rho \int 4\pi r^2 (g(r) - 1) \frac{\sin 2\pi r s}{2\pi r s} dr \quad (4)$$

where $\rho = cN_a/M$ is the number of particles per unit of volume, c the particle concentration (g/cm^3), N_a the Avogadro's number and M the particle molecular weight (g/mol).

The X-ray structure factor at the s -origin, $S(c, 0)$, is related to the osmotic pressure Π of the particle solution [8]. For solutions of particles in repulsive (attractive) regime, $S(c, 0)$ is smaller (larger) than 1. It is given by:

$$S(c, 0) = \frac{RT}{M} \left(\frac{\partial \Pi}{\partial c} \right)^{-1} \quad (5)$$

where R the gas constant, $8.31 \text{ J}\cdot\text{mol}^{-1}\cdot\text{K}^{-1}$, T the absolute temperature in K , M the particle molecular weight and Π the osmotic pressure described by [12]:

$$\frac{\Pi}{cRT} = \frac{1}{M} + A_2 c + (\text{terms of order } c^2) \quad (6)$$

A_2 depends on the interaction pair potential $U(r)$ between particles in solution by the expression:

$$A_2 = \frac{2\pi N_a}{M^2} \int_0^{+\infty} \left(1 - \exp\left(-\frac{U(r)}{k_B T}\right) \right) r^2 \cdot dr \quad (7)$$

with $U(r) = +\infty$ for $r < \sigma$, r being the interparticle distance, in g/mol and σ the particle diameter and N_a is the Avogadro's number.

A_2 is positive for repulsive interactions and negative for attractive ones and is expressed in $\text{mol}\cdot\text{cm}^3\cdot\text{g}^{-2}$.

3. EXPERIMENTAL BACKGROUND

3.1 Sample preparation

BPTI (6511 Da, $pI \approx 10.5$) was supplied purified as a lyophilized powder by Bayer and used as received without further purification. Proper amounts of BPTI and salts (NaCl , KSCN , $(\text{NH}_4)_2\text{SO}_4$) were dissolved in pure water (ELGA UHQ reverse osmosis system) to obtain stock solutions needed for crystallization trials and SAXS experiments. The different solutions were buffered with acetic acid to 80mM, adjusted to pH 4.5 with NaOH (1M) and filtered through $0.22\mu\text{m}$ Millipore filters. The BPTI concentration was controlled by optical density measurements using an extinction coefficient of $0.786 \text{ cm}^2\cdot\text{mg}^{-1}$ at 280nm.

UOX (homotetramer of 128 kDa, $pI \approx 7.5$) was supplied in solution with excess of inhibitor by Sanofi-Synthelabo. The excess inhibitor was removed by gel filtration chromatography. Several stock solutions of UOX were prepared in buffers at different pH (50mM Tris pH 7.5, 8.0, 8.5, 9.0, 10mM

Na borate pH 8.7 and 10mM sodium carbonate pH 10.5). PEG solutions (PEG 3350, 8000 and 20000 from Hampton research) and salt solutions (NaCl, NaCH₃CO₂ from Sigma) were prepared at respectively 40 % w/v for PEGs and 2 M for salt and buffered at appropriate pH. The concentration was determined by optical density measurements at 280nm using an experimental extinction coefficient of $2.2 \pm 0.1 \text{ cm}^2.\text{mg}^{-1}$ (for the complex protein-inhibitor). All solutions were filtered on Millex-LCR filters 0.45 μm (from Millipore).

3.2 SAXS experiment

X-ray scattering patterns were recorded on the small-angle scattering beamline D24 at LURE (Orsay). The instrument, the data acquisition system and the thermostated cell under vacuum used for these experiments have already been described [13-15]. The wavelength of the X-rays was 1.488 Å (K-edge of Ni). The minimum sample volume to be injected in the cell was about 50 μl . The sample to detector distances varied from 1.60 to 2.20 m as a function of the protein studied. Several successive frames with duration of 100 or 200s each, according to protein concentrations and sample composition, were recorded for each sample and corresponding buffer. The curves were scaled to the transmitted intensity measured by scattering of a strong scatterer (e.g. black carbon). After subtraction of the appropriate buffer, the scattering curves were normalized to the protein concentration before plotting and analyzed either in term of form factor or in term of interactions.

3.2.1 Simulation procedure

For ideal solutions (i.e. diluted solutions), when crystallographic coordinates of the protein studied are available in the Protein data bank, the CRY SOL program [16] can be used to calculate scattering form factors and to determine the different species in solution in the case of polydisperse solutions.

For BPTI, calculated form factors for monomer and decamer were obtained using CRY SOL from a set of crystallographic coordinates (PDB entry 1BHC; [17]). The experimental curves can be fitted by a linear combination of monomers and decamers as described by Hamiaux [18]. Two main parameters were taken into account for the fitting procedure: the protein quantity and the percentage of decamers.

3.2.2 Second virial coefficient

For concentrated monodisperse solutions of macromolecules in presence of weak interactions, the scattering curves were analyzed in terms of structure factor. The second virial coefficient was calculated from the structure factor at zero s-origin from:

$$\frac{1}{S(c,0)} = \frac{I(0,0)}{I(c,0)} = 1 + 2MA_2c + \dots \quad (9)$$

If the term $2MA_2$ is small ($\ll 1$), the expansion in powers of c of $S(c,0)^{-1}$ can be limited to the second virial coefficient and linearized.

4. STRUCTURE OF BPTI IN SOLUTION PRIOR TO CRYSTALLIZATION

4.1 Solubility

After the pioneering studies on Lysozyme, a small protein of 14300 Da often used as model system, for which it was shown a close correlation between the decrease in solubility and the increase in attractive interactions when salts are added [3, 19], other biological systems have been studied by scattering techniques to determine crystallization conditions and to characterize crystal growth mechanisms. In the case of BPTI, solubility curves have previously been determined in different salts [5, 20].

For BPTI at pH 4.5 at 20°C, the effectiveness of SCN^- as crystallization agent is higher than that of Cl^- , which is higher than that of SO_4^{2-} (Figure 2).

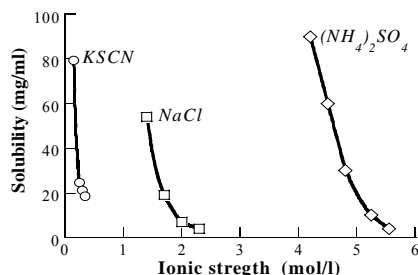
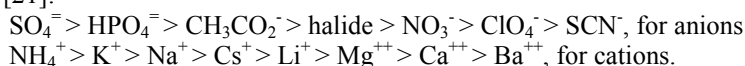


Figure 2. Comparison of BPTI solubility curves with KSCN, NaCl, and $(\text{NH}_4)_2\text{SO}_4$ at pH 4.5 at 20°C

As it was observed for Lysozyme, a basic protein ($\text{pI}=11.3$), the effectiveness of salts to decrease BPTI solubility follows the reverse order of the lyotropic Hofmeister series. The Hofmeister lyotropic salt series is described by [21]:



In the case of acidic proteins [22, 23], it was shown that the effectiveness of salts to decrease the protein solubility follows the direct Hofmeister series.

4.2 BPTI form factor in solution

According to the solubility curves of BPTI (Figure 2), SAXS experiments were performed at pH 4.5 at 20°C in KSCN from 0 to 350mM, in NaCl from 0.1 to 1.4M and in $(\text{NH}_4)_2\text{SO}_4$ at 1.25M. In every cases, the addition of salt clearly modifies the BPTI polydispersity at concentration below but close to the solubility. It is noteworthy that the solubility of BPTI at 20°C pH 4.5 is 18.5mg/ml in 350 mM KSCN, 54mg/ml in 1.4M NaCl and more than 90mg/ml in 1.25M $(\text{NH}_4)_2\text{SO}_4$ [5, 20].

Because of this polydispersity as the salt concentration increases, it was not possible to analyze the scattering intensities in term of second virial coefficient. Nevertheless SAXS measurements have been analyzed in term of radius of gyration by using the Guinier approximation (Eq. 2). In Figure 3, the BPTI radius of gyration increases from about 13Å to 24.5Å when its concentration increases as a function of salt concentration, corresponding to an oligomerization.

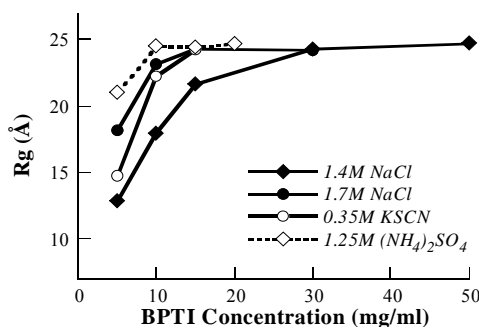
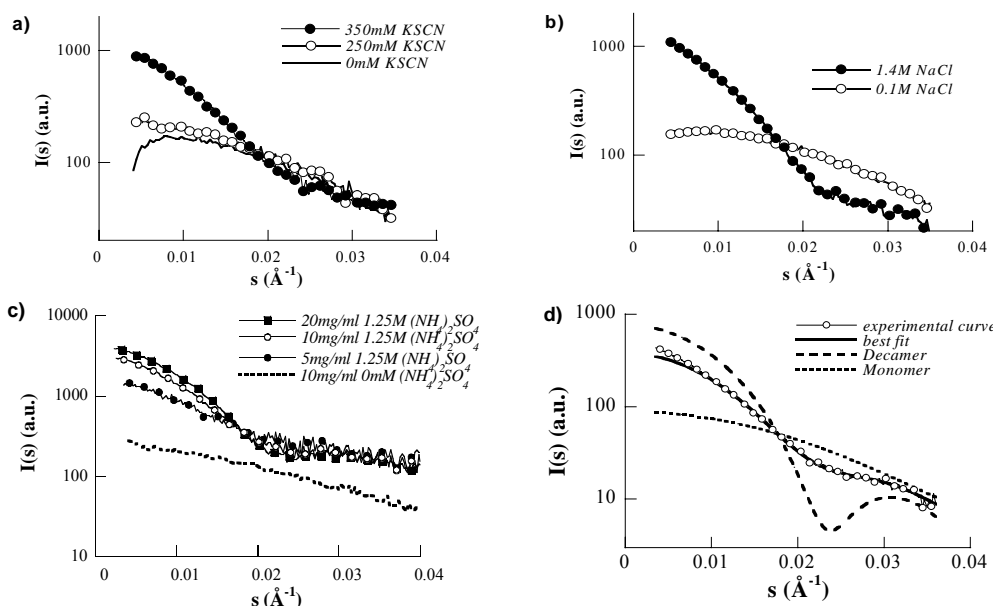


Figure 3. BPTI radius of gyration in different salts at pH 4.5

The experimental scattering patterns (Figures 4a, b, c) clearly show a drastic change of the form factor whatever the salt. This change has been analyzed by a combination of calculated scattering curves of monomer and decamer of BPTI (Figure 4d) [24, 18].



Figures 4. Experimental BPTI SAXS patterns at different concentrations in KSCN (a), NaCl (b) and $(\text{NH}_4)_2\text{SO}_4$ (c) at pH4.5 and 20°C. **d)** Calculated curves computed with CRY SOL for monomer and decamer of BPTI corresponding to SAXS experimental curve of BPTI 15mg/ml in 350 mM KSCN pH 4.5 at 20°C, and best fit considering a mixture of 69.4% of monomers and 30.6% of decamers [24].

By correlating phase diagram and SAXS experiments in the different salts, we observed an oligomerization of BPTI as a decamer as the concentration of salt increases close to the solubility curve. Thus BPTI needs to be in a decameric state to crystallize. Recent results have shown that the nucleation kinetic is strongly related to the decamer quantity in solution [24] and that crystals grow by addition of decamers. This was confirmed by Atomic Force Microscopy (not shown), which makes it possible to measure the step height of 70Å of a growing BPTI crystal, corresponding to the BPTI decamer diameter in the crystal packing. No evidence of any intermediate species was found [25] as confirmed recently, by magnetic relaxation dispersion [26].

5. URATE OXIDASE: A MODEL OF DEPLETION ATTRACTION

5.1 Structure in solution

To generalize results obtained with small proteins to other biological systems, we have extended SAXS and crystallization studies to Urate oxidase. The experimental form factor of UOX in 10mM Na Carbonate pH 10.5 was fitted with the calculated CRY SOL form factor by the UOX tetramer obtained from the crystallographic coordinates (PDB entry 1UOX) (Figure 5a). In sodium carbonate, the UOX scattering intensity decreases as the concentration of protein increases without changes of the form factor (Figure 5b), visualized in Log scale (Insert in Figure 5a). This variation of the scattering intensity characterizes repulsive interactions between macromolecules in solution. The second virial coefficient calculated from the scattering intensity at zero s-origin is $+0.4 \cdot 10^{-4} \text{ mol.ml.g}^{-2}$.

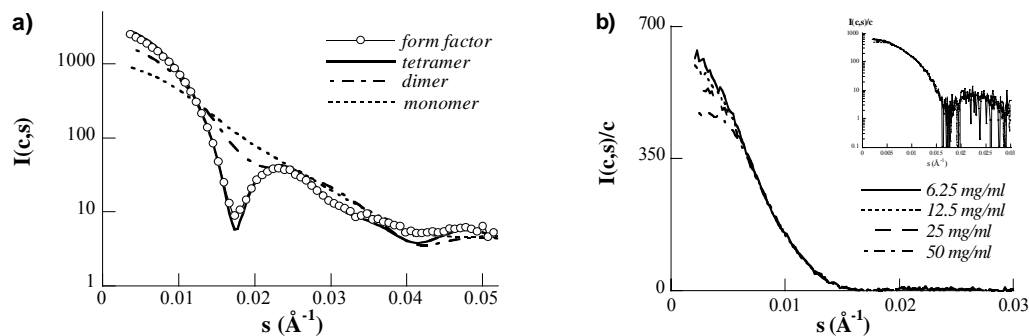


Figure 5. a) UOX form factor and fitted atomic models (PDB entry: 1UOX) for the monomer, the dimer and the tetramer of urate oxidase using the program CRY SOL. b) SAXS patterns of UOX as a function of protein concentration in 10mM Na Carbonate pH 10.5. The insert is in Log scale.

5.2 Interactions in solution

5.2.1 Salt effect

Previous results have shown that the protein charges can be screened by addition of salt, leading to more attractive interactions [1-3]. We therefore increased the ionic strength of sodium carbonate in the protein solution. X-ray scattering intensities of UOX at 25mg/ml in 10, 100 and 300mM Na carbonate pH 10.5 were measured.

It did not show a modification of interactions in solution but a drastic change in the form factor at 300 mM Na carbonate, which corresponds to a change in the quaternary structure of the enzyme. The intensity near the origin, which is proportional to the particle molecular weight, was reduced by about a factor 2 from the solution in 10mM to the solution in 300mM (Figure 6a), indicating that UOX lost its tetrameric structure for a dimeric structure [27].

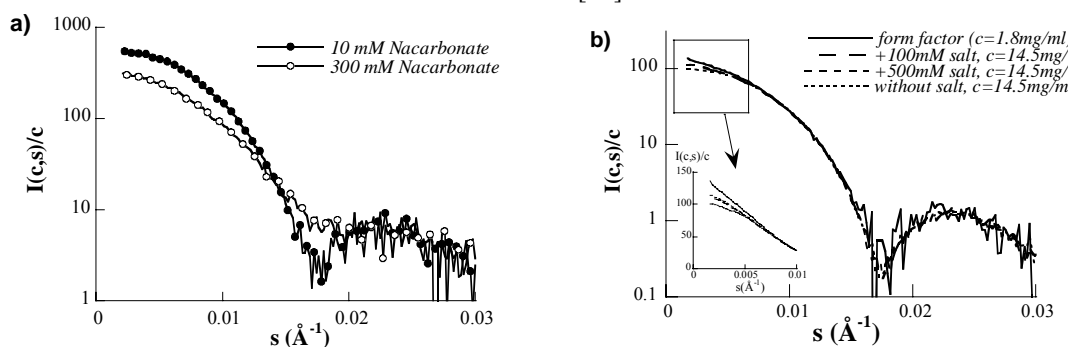


Figure 6. a) Form factor of urate oxidase from *Aspergillus flavus* in 10 mM and 300mM Na carbonate pH 10.5; b) SAXS patterns of UOX in Na acetate pH 10.5.

Some experiments were performed with addition of other salts at pH=10.5 far from the protein isoelectric point ($pI \approx 7.5$). Since the pH of the solutions studied were above the UOX isoelectric point, sodium acetate and sodium sulfate were chosen within the direct Hofmeister series, to be a priori the most efficient salts to induce attractive interactions and protein crystallization [22, 23]. At pH 10.5, adding sodium acetate (Figure 6b), whatever their concentrations up to 500mM, did not bring the solution into an attractive regime. The effect of salt addition was progressive until 100mM, which corresponds to the concentration necessary to screen the charges on the surface of the molecule. There was neither differences nor additional effects between 100mM and 500mM salt (Insert in Figure 6b)

5.2.2 pH and temperature effects

Since there was no change from repulsive to attractive interactions by a simple addition of salt as it was with small globular proteins, we decided to vary the pH closer to pI, while remaining in the range of the enzyme stability. Between pH 10.5 and pH 7.5, the UOX scattering intensity increased as pH became closer to pI but interactions remained repulsive; the second virial coefficient varies from $+0.86 \times 10^{-4} \text{ mol.ml.g}^{-2}$ to $+0.17 \times 10^{-4} \text{ mol.ml.g}^{-2}$ (Figure 7a).

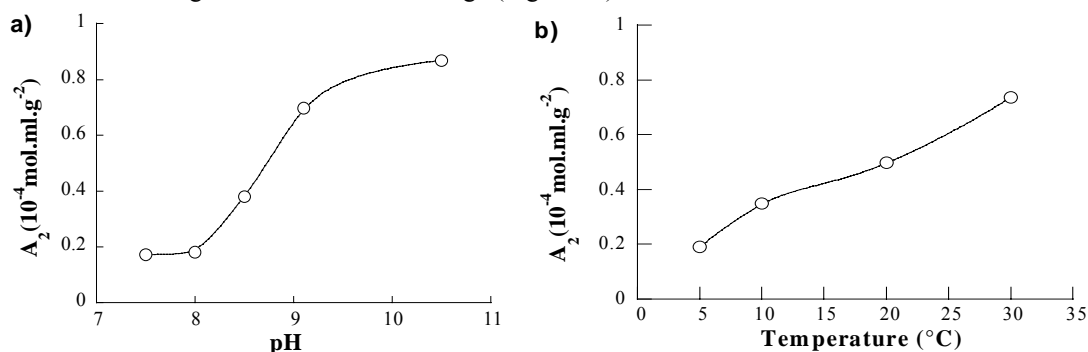


Figure 7. Variation of the second virial coefficient of UOX a) as a function of pH at 20°C, b) as a function of temperature in Na borate buffer pH 8.7.

SAXS experiments were also performed on a large range of temperature from 5°C to 30°C, in the limit of the protein stability, at a constant pH close to the isoelectric point ($pI \approx 7.5$), where the repulsive component was weak. Since the Tris buffer was very sensitive to variations of temperature ($dpK_a/dT = -0.028$, [28]), we used a 50mM sodium borate buffer, whose pH is known to be less temperature-dependant ($dpK_a/dT = -0.008$). A_2 values were determined from SAXS experiments as a function of UOX concentration at each temperature (Figure 7b). The second virial coefficient remained positive, while sharply increasing with the temperature. An increase of scattering intensity when the temperature decreases was already observed with small biological systems (Lysozyme [1], γ -crystallin [29]) but not with large ones (ATCase [2] or α -crystallin [30]). This effect is mainly due to Van der Waals attraction, which is more sensitive to temperature.

In contrast to the case of small soluble proteins, adding salt or decreasing temperature was found to be less effective to induce attractive interactions with UOX whatever the pH of the solution.

5.2.3 Non absorbing polymer effect

The addition of a non absorbing polymer (Polyethylene glycol) is known to induce a depletion attraction, originally described in the case of colloid-polymer mixtures [31, 32] and which was then described in the case of protein-polymer mixtures [33]. The depletion attraction can be simply explained for an ideal polymer solution (Figure 8).

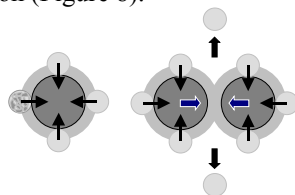


Figure 8. Model of depletion attraction

Molecules of polymer, characterized by a radius of gyration R_g , and colloids cannot mutually interpenetrate. The centers of polymers are therefore excluded from a region of thickness R_g around each colloidal particle, called the depletion zone. When two colloid particles come sufficiently close

to each other, their depletion zones can overlap and the free volume accessible to the polymer molecules increases, leading to a gain in entropy of the system. Thermodynamically, it is therefore more favorable for the polymer that the colloidal particles get closer, which corresponds to an attractive interaction, function of the polymer mass and concentration [34-36]. This model remains valid as long as molecules of polymer do not overlap.

PEG concentration and size effects were studied on the UOX interactions in solution. SAXS experiments were performed at pH 8.5, where the repulsion is the lower, with three different PEGs: 3,350 Da, 8,000 Da, 20,000 Da. The increase of the scattered intensity observed at small angles ($s < 0.005 \text{ \AA}^{-1}$) with the increase of protein concentration was indicative of attractive interactions between particles (Figure 9a). Expressed in terms of second virial coefficient (Figure 9b), we observed that, whatever the size of PEG, it was possible to reach to a negative second virial coefficient corresponding to an attractive regime, by increasing the concentration or the molecular weight of polymer.

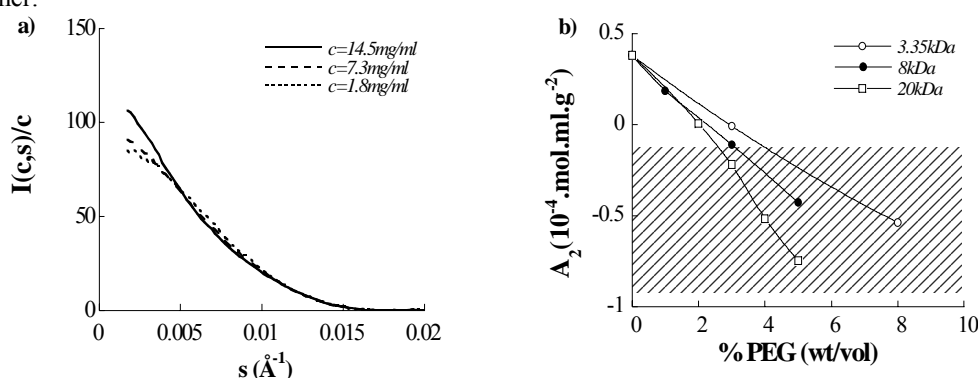


Figure 9. a) UOX SAXS patterns in 8% PEG 3350 at pH 8.5 as a function of protein concentration; b) Second virial coefficient of UOX in three different PEGs at pH 8.5

This result highlights the correlation between interactions in solution and solubility since Atha and Ingham [37] showed that protein solubility decreases when the polymer molecular weight and concentration increase. In contrast to the case of salt, where no crystal was observed after several weeks at room temperature, UOX crystals grew in a few days from 15mg/ml solutions of enzyme at pH 8.5 with different percentages of the three PEGs [7]. By correlating the different crystallization trials of urate oxidase in the three PEGs at pH 8.5 with the second virial coefficient, we observed that the nucleation rate in the different crystallization drops follows the variation of A_2 and that the enzyme crystallized in a very narrow range of A_2 : $-0.80 < A_2 (10^{-4} \text{ mol.ml.g}^{-2}) < -0.10$ (hatched area in Figure 9b). The upper and lower limits of A_2 are those determined from growing crystals in a usual range of protein concentration (10 to 30mg/ml). In this protein concentration range, higher concentrations of PEG led either to liquid-liquid phase separations, which can give crystals or amorphous precipitation.

6. DISCUSSION

The BPTI study has shown that salt alone is efficient to decrease solubility and to get crystals. During the crystal growth mechanism by SAXS, we observed the BPTI decamerization, which is one condition to get crystals of BPTI (Figure 10).

The UOX study has shown that the determination of the second virial coefficient A_2 from the SAXS measurements is a non destructive method to predict crystallization conditions. Studies of large macromolecules have confirmed the important crystallizing power of a broad range of PEG for large proteins and that the addition of monovalent salts alone is often unable to induce attraction leading to crystallization.

It is noteworthy that in the case of BPTI, temperature has an important effect on solubility [5, 20] whereas it has almost no effect on UOX solubility in PEG [27].

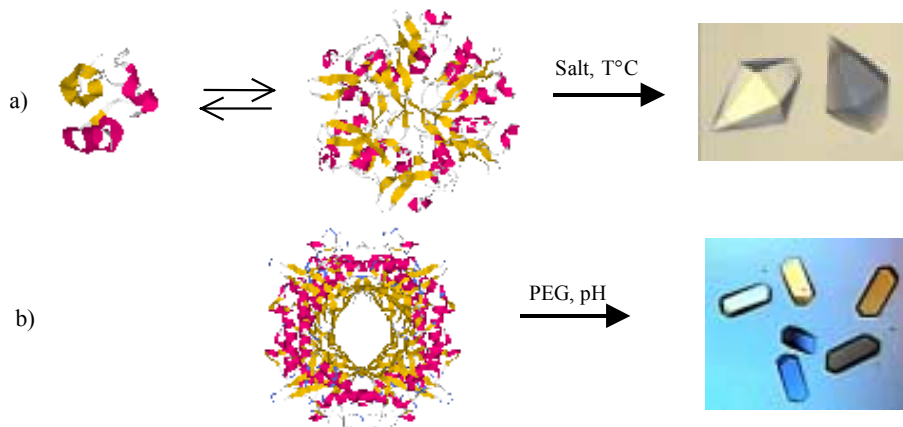


Figure 10. a) Decamerization mechanism of BPTI with addition of salt leading to crystal growing; b) Crystallization of Urate oxidase with addition of PEG.

7. CONCLUSION

Results presented in this article have shown that Small Angle X-ray Scattering is a useful and effective tool to characterize protein structure in solution prior to crystallization and to characterize protein-protein interactions in solution in order to determine crystallization conditions, instead of lengthy determination of phase diagrams and solubility curves.

Acknowledgements

We thank Bayer A.G. (Wuppertal, Germany) for providing us with BPTI and Mohamed El Hajji (Sanofi-Synthelabo) for providing us with Urate oxidase. We thank Dr P. Vachette and Dr J. Perez (LURE-CNRS, Orsay), for their help and advice in the SAXS experiments.

References

- 1 F. Bonneté, S. Finet, A. Tardieu, *J. Crystal Growth* 196, 403 (1999).
- 2 M. Budayova, F. Bonneté, A. Tardieu, P. Vachette, *J. Crystal Growth* 196, 210 (1999).
- 3 A. Ducruix, J.P. Guilloteau, M. Riès-Kautt, A. Tardieu, *J. Crystal Growth* 168, 28 (1996).
- 4 A. George, W.W. Wilson, *Acta Cryst. D50*, 361 (1994).
- 5 S. Lafont, S. Veesler, J.P. Astier, R. Boistelle, *J. Crystal Growth* 173, 132 (1997).
- 6 M. Muschol, F. Rosenberger, *J. Chem. Phys.* 103, 10424 (1995).
- 7 D. Vivarès, F. Bonneté, *Acta Cryst. D58*, 472 (2002).
- 8 A. Guinier, G. Fournet, in *Small angle scattering of X-rays*, Edited by Wiley (New York, 1955).
- 9 P. Lindner, T. Zemb, in *Neutron, X-ray and light scattering: introduction to an investigative tool for colloidal and polymeric systems*, Edited by North-Holland Delta Series (Amsterdam, 1991).
- 10 A. Tardieu, in *Neutron and Synchrotron Radiation for Condensed Matter Studies*, edited by Springer-Verlag: Les éditions de Physique (France, 1994), p 145.
- 11 P. Vachette. in *Proceedings of the International school of physics "Enrico Fermi"* (1996), p. 269.
- 12 Eisenberg H., in *Biological Macromolecules and Polyelectrolytes in solution*, Edited by Clarendon Press. (Oxford, 1976).
- 13 C. Boulin, R. Kempf, M.H.J. Koch, S.M. McLaughlin, *Nucl. Instrum. and Meth.* A249, 399 (1986).

- 14 C. Depautex, C. Desvignes, P. Feder, M. Lemonnier, R. Bosshard, P. Leboucher, D. Dageaux, J.P. Benoit, P. Vachette, in LURE: rapport d'activité pour la période Août 1985-1987, edited by documentation CEN Saclay, (1987).
- 15 J.M. Dubuisson, T. Decamps, P. Vachette, *J. Appl. Cryst.* 30, 49 (1997).
- 16 D. Svergun, C. Barberato, M.H.J. Koch, *J. Appl. Cryst.* 28, 768 (1995).
- 17 C. Hamiaux, T. Prangé, M. Ries-Kautt, A. Ducruix, S. Lafont, J.P. Astier, S. Veessler, *Acta Cryst. D55*, 103 (1999).
- 18 C. Hamiaux, J. Perez, T. Prange, S. Veessler, M. Ries-Kautt, P. Vachette, *J Mol Biol* 297, 697 (2000).
- 19 M. Ries-Kautt, A. Ducruix, *J. Biol. Chem.* 264, 745 (1989).
- 20 S. Lafont, S. Veessler, J.P. Astier, R. Boistelle, *J. Crystal Growth* 143, 249 (1994).
- 21 F. Hofmeister, *Arch. Exp. Pathol. Pharmacol.* 24, 247 (1888).
- 22 C. Carbonnau, M. Ries-Kautt, A. Ducruix, *Protein Sci.* 4, 2123 (1995).
- 23 S. Veessler, S. Lafont, S. Marcq, J.P. Astier, R. Boistelle, *J. Crystal Growth* 168, 124 (1996).
- 24 S. Grouazel, J. Perez, J.-P. Astier, F. Bonneté, S. Veessler, *Acta Cryst. D58*, 1560 (2002).
- 25 M. Budayova-Spano, F. Bonneté, J.P. Astier, S. Veessler, *J. Crystal Growth* 235, 547 (2002).
- 26 M. Gottschalk, K. Venu, B. Halle, *Biophys J* 84, 3941 (2003).
- 27 D. Vivarès, "Interactions en solution et cristallisation de l'urate oxydase", Thèse de Doctorat, Université Paris 6, Paris, (2003).
- 28 R.J. Beynon, J.S. Easterby, in *Theory of buffer action*, Edited by B.S. Publishers (Oxford.1996).
- 29 M. Malfois, F. Bonneté, L. Belloni, A. Tardieu, *J. Chem. Phys.* 105, 3290 (1996).
- 30 S. Finet, A. Tardieu, *J. Crystal Growth* 232, 40 (2001).
- 31 S. Asakura, F. Oosawa, *J. Chem. Phys.* 22, 1255 (1954).
- 32 A. Vrij, *Pure Appl. Chem.* 48, 471 (1976).
- 33 H. Mahadevan, C.K. Hall, *AIChE J.* 36, 1517 (1990).
- 34 A.M. Kulkarni, A.P. Chatterjee, K.S. Schweizer, C.F. Zukoski, *J. Chem. Phys.* 113, 9863 (2000).
- 35 H.N.W. Lekkerkerker, *Physica A* 244, 227 (1997).
- 36 R. Tuinier, G.A. Vliegthart, H.N.W. Lekkerkerker, *J. Chem. Phys.* 113, 10768 (2000).
- 37 D.H. Atha, K.C. Ingham, *J. Biol. Chem.* 256, 12108 (1981).